stored energy of ³ 1kJ, and peak discharge current of ³ 100kA) comes due to micro-pinching of the plasma in the discharge gap to a high temperature of 1-10keV and at high density ~ 10^{22} – 10^{23}cm^{-3}. It will be interesting if such a hard X-ray source operates as a low energy compact device. Recent experiments performed at CAT in collaboration with P. N. Lebedev Physical Institute, Moscow, have shown intense multi-keV X-ray generation in a low-energy (£ 20J, electrical) moderate-current (~ 10kA) vacuum discharge initiated by short duration (multi-picosecond) laser pulses.

A schematic of the experimental set-up is shown in fig. L.5.1. The vacuum diode consists of a planar titanium plate as a cathode and a conical point-tip titanium anode, kept at a separation of ~ 3mm. The anode was biased to a voltage up to +20kV using a dc power supply and a low inductance 100nF capacitor. The inductance of the discharge circuit was ~ 0.15mH. The whole set-up was kept inside a chamber evacuated to a pressure of ~ 5 x 10^{-5} torr. The discharge was triggered by producing a plasma on the cathode using laser pulses of ~ 5mJ energy, 27ps full-width at half-maximum duration from an Nd:glass laser (wavelength: 1.054 mm). The laser beam was incident on the cathode at an angle of 45^0 to the cathode normal.

Intense K-shell (Ka: hn » 4.51keV) X-ray emission was observed from the titanium anode tip due to its bombardment by the accelerated electrons extracted from the expanding cathode plasma. This X-ray emission occurs in the form of two or three pulses, each of 20-30 ns duration, occurring up to ~ 100ns from the time of triggering. The number of Ka photons is estimated to be » 6 x 10^{10} photons per shot, comparable to that for the nanosecond pulse laser-driven vacuum diode X-ray source [A. Moorti et al. Pramana - J. Phys. 63, 1031, 2004]. An evidence of a much harder X-ray component (hn > 100keV) was also seen from the flooding of

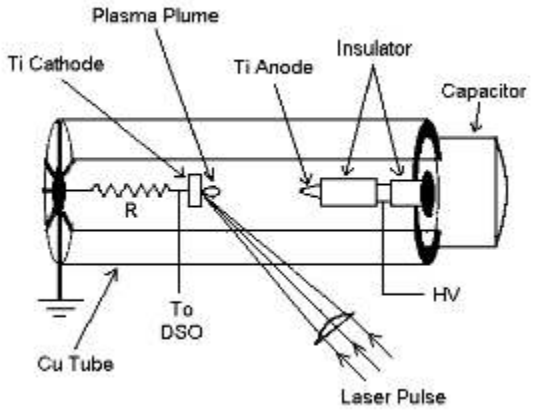

Fig L.5.1 *Schematic of the experimental set-up.*

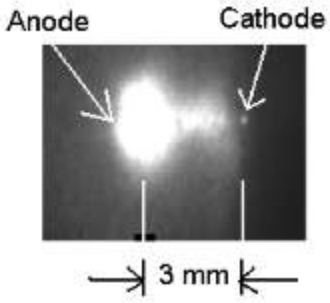

Fig L.5.2 *Pin-hole image of the discharge gap.*

micro channel plate detector filtered through 10mm thick copper disc. Hence the discharge gap was imaged at a lower anode voltage of ~ 5kV using an X-ray pin-hole camera filtered with a formvar filter of 0.3mm thickness (photon energy for 1/e transmission ~ 100eV). The image of the discharge gap (fig. L.5.2) clearly shows pinching of the plasma near the cathode [A. Moorti et al. J. Appl. Phys. to appear in February1, 2005 issue]. This pinching effect occurring in the cathode plasma jet expanding with a free boundary is different from the high-current discharges in which the pinching occurs in the plasma column bound by the electrode surfaces. Detailed measurements of hard X-ray emission will be carried out.

(Contributed by: Anand Moorti (moorti@cat.ernet.in)
and P. A. Naik)

L.6 Development of fiber optic based optical coherence tomography setup for in-vitro and in-vivo imaging of biological tissues

Optical coherence tomography (OCT) is a very attractive technique for real time depth resolved cross-sectional imaging of biological tissues and can provide micrometer-scale resolutions. OCT relies on the principle of low coherence interferometry, wherein light from a broadband source backscattered from a sample is mixed with the reference light using Michelson interferometer geometry. Interference takes place only when the sample arm path length matches exactly the reference arm path within the coherence length of the source. This allows probing different layers of the sample. Two-dimensional cross sectional imaging is achieved by performing successive axial measurements at different transverse positions. Heterodyne detection is used to detect the weak interference signal that has the signatures of the sample layer being investigated. OCT is being increasingly used in various clinical areas like ophthalmology, gastroenterology, dermatology, etc. A single mode fiber optic based optical coherence tomography system has been developed and used for in-vitro and in-vivo imaging of

biological tissues. The set up, makes use of super luminescent diode sources with center wavelengths of ~ 840nm and ~ 1305nm. The diode output was coupled into a fiber optic based Michelson interferometer by use of a 3-dB bi-directional fused fiber coupler designed for the wavelength used. The light beam in the sample arm was collimated and focused on to the sample with a microscopic objective.

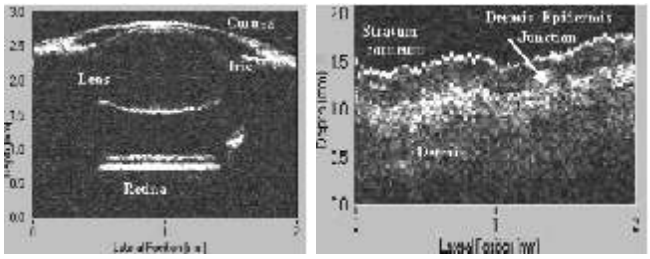

(a) (b)

Fig L.6.1 *(a) Image of fish eye showing different layers (b) In-vivo image of human skin (finger-pad)*

The reference mirror was mounted on a linear translation stage and translated back and forth with a uniform velocity. The light reflected from both the sample and reference arms was detected by a photodiode and the resulting interferogram was demodulated using a lock-in amplifier. The interferogram envelope was digitized and acquired in a PC using a data acquisition card. Lateral scanning was done using a stepper motor. The axial and lateral resolutions of the setup in free space were ~11mm and 27mm respectively at 840 nm and ~25ìm and 40ìm respectively at 1305mm. The image of a fish eye acquired with the 1305nm set up is shown in fig. L.6.1(a). The different layers of the eye like the cornea, iris, lens and the retina can be clearly seen. The set up has also been used for in–vivo imaging of human skin (fig. (b)). The stratum corneum and the epidermis-dermis junction are clearly visible. Real time imaging set up using a rapid scanning optical delay line is being assembled and should prove useful for dermatological applications.

(Contributed by: K Divakar Rao and P. K. Gupta: pkgupta@cat.ernet.in)

L.7 Interaction dynamics of RBC in optical tweezers : prospects for microfluidic actuations and diagnosis of malaria

There exists considerable current interest in understanding the interaction of objects of different shape with the trap beam in an optical tweezers set up. Apart from furthering basic understanding of trapping forces such interactions can also be used for construction of micromotors and other devices. Red blood cells provide a good model system for this purpose because their shape can be conveninetly modulated by a change in the osmolarity of the suspension in which these are placed. We have investigated the dynamics of the interaction of RBC with trap laser beam at different osmolarity of the suspension and power of the trap beam. RBCs suspended in isotonic buffer (~300 mOsm/kg) are discotic and when optically tweezed they reorient and align with their edge length along the trap laser propagation direction. The time required for a RBC to switch from initial horizontal position to the vertical orientation was found to decrease with both an increase in the trapping power and osmolarity of the buffer. At 85 mW trap beam power the time required varied from 240 ms to 120 ms for a change in osmolarity from 300 mOsm/Kg to 800 mOsm/Kg. The vertically oriented RBCs take a longer time to return to the horizontal orientation when the trap beam is put off. Faster reorientation to horizontal plane (~ 0.2 s) could be achieved by subjecting the RBC to a burst of radiation pressure from a focused pulsed laser or to a viscous drag on its surface closer to the cover slip by translation of the microscope stage. These experiments also showed that contrary to a recent report there does not occur any folding of the RBC membrane when it is optically tweezed. The switching of RBC from horizontal to vertical plane or vice-versa can be utilized as an optically controlled valve. For this application use of a linearly polarized trap beam offers an added advantage because then the RBC orients with its plane oriented along the plane of polarization of the trapping beam. By rotating the plane of polarization of the trap beam the disk can be oriented at different angles about the trap beam axis.

More interestingly, we found [S. K. Mohanty, A. Uppal, P. K. Gupta, *Biotechnol. Lett.* 26, 971-974 (2004)] that in hypertonic buffer medium (osmolarity > 800mOsm/kg), the meniscus shaped normal RBC rotates when optically trapped with trap beam power beyond ~ 40mW (fig.L.7.1). This arises due to the torque generated on the cell by transfer of linear momentum from the trapping beam. For a given osmolarity the rotational speed was observed to increase super-linearly with an increase in trap beam power. RBC having malaria parasite in it (as confirmed by fluorescence of acridine orange stain) does not rotate. Even more significant is the fact that the rotational speed of other RBCs from malaria-infected blood sample, which did not show acridine orange fluorescence, was an order of magnitude smaller and increased much slower with an increase in trap beam power as compared to normal cells. We could screen around 40 RBCs/min by making the cells flow through the trapping point at a velocity of ~ 10 mm/sec. When a flowing RBC struck a trapped RBC, the trapped RBC was thrown out by the collision and the other RBC gets trapped and starts rotating if normal. Higher-screening rates are possible by increasing the flow rate of RBCs and by increasing the number of traps in an array